

## Swelling and Structural Changes of Oppositely Charged Polyelectrolyte Gel–Mixed Surfactant Complexes

Henry S. Ashbaugh\* and Björn Lindman

Physical Chemistry 1, Center for Chemistry and Chemical Engineering, Lund University, Box 124, S-221 00 Lund, Sweden

Received September 6, 2000

Revised Manuscript Received December 19, 2000

### Introduction

Polyelectrolyte and hydrogel complexation with oppositely charged surfactants provides a simple route for constructing ordered materials whose structures reflect the underlying surfactant mesophases.<sup>1</sup> The association between a hydrogel and oppositely charged surfactant can best be viewed as a polymer-induced micellization at concentrations well below the critical micelle concentration (cmc) of the surfactant,<sup>2</sup> resulting in a collapse in the volume of the initially swollen gel and concomitant ordering of the bound surfactant aggregates. Novel structures unavailable to the surfactant alone can arise from synergistic interactions with the hydrogel and the imposed geometric constraints of the network.<sup>3</sup> These complexes have a host of applications including tailored rheological and material properties, models of biological systems, gene and drug delivery vehicles, and responsive systems. While a variety of gel–surfactant mesostructures have been observed including cubic, hexagonal, and lamellar, the relationship between the complex structures, experimental conditions, and chemical identities of the constituents is not straightforward.<sup>3–8</sup>

In addition to hydrophobic associations between surfactant tail groups, electrostatic interactions certainly play an important if not dominant role in determining polyelectrolyte–surfactant complex structures. Chu and co-workers, for example, observed a progression from primitive cubic, to face-centered cubic, to hexagonally close packed, to amorphous structures for alkyltrimethylammonium-*co*-polymethacrylic acid/*N*-isopropylacrylamide gel complexes with increasing *N*-isopropylacrylamide monomer fraction, i.e., decreasing gel charge density. In this Note, we examine how the structure of an oppositely charged surfactant–polyelectrolyte complex evolves with decreasing micelle surface charge density. In particular, we consider the association of nonionic/cationic surfactant mixtures of octaethylene glycol monododecyl ether (C<sub>12</sub>E<sub>8</sub>) and dodecyl trimethylammonium bromide (DTAB) with lightly cross-linked sodium polyacrylate (cPA) hydrogels. This mixed surfactant–hydrogel system has previously been studied using detailed absorption isotherm measurements, demonstrating that the cPA–mixed surfactant interactions are highly cooperative, indicative of micellization within the gel.<sup>9</sup> Herein we show that the nonionic surfactant isotropically swells the neat DTA<sup>+</sup>–cPA complex and diminishes long-range polycrystalline cubic

order as determined by small-angle X-ray scattering (SAXS) at low surfactant concentrations. More interestingly, with increasing nonionic surfactant concentration, the gel volume swells in a stepwise manner on length scales greater than the intermicellar spacing, suggesting heterogeneous micelle-rich and micelle-lean regions distributed throughout the gel.

### Experimental Section

Cross-linked sodium polyacrylate gels (cPA) were prepared by free radical copolymerization of acrylic acid monomer (Aldrich) and 0.9 mol % *N,N*-methylenebis(acrylamide) cross-linker (Sigma) as described in ref 9. Then, 24 h after initiation of the polymerization, the gels were placed in a large excess of concentrated NaOH to deprotonate the acid monomers. The gels were subsequently placed in a 0.01 mM NaOH bath, which was changed every other day for more than a month to maintain pH 9 and wash away unreacted species. In the bath, the gels swelled to several times their initial volume, such that the monomer concentration was 21.1  $\mu\text{mol/g}$  of swollen gel (0.198 wt % monomer).

Swollen gel samples were cut and placed in dodecyl trimethylammonium bromide (DTAB)/octaethylene glycol monododecyl ether (C<sub>12</sub>E<sub>8</sub>) surfactant mixtures of known composition at pH 9 prepared with degassed Millipore water. The mass ratio of the initial swollen gel to external surfactant solution was 1:8. All the samples were kept in capped vials sealed with Parafilm and equilibrated for more than a month at 25 °C. Sixteen mixed DTAB (TCI)/C<sub>12</sub>E<sub>8</sub> (Nikkol) solutions of varying C<sub>12</sub>E<sub>8</sub> concentration were prepared. The concentration of DTAB in the initial solutions was fixed at 10 mM, such that the total cationic surfactant is nearly four times that required to saturate the cPA network. The concentration of C<sub>12</sub>E<sub>8</sub> in the initial solutions was varied from 0 to 30 mM in 2 mM increments, corresponding to a maximum C<sub>12</sub>E<sub>8</sub> surfactant fraction of 0.75.

After equilibration for more than a month, the collapsed gels were removed from their vials and carefully weighed after blotting excess water from their surfaces with filter paper. The volume collapse ratio  $\alpha$ , defined as the ratio of the final to initial gel mass ( $V_f/V_i$ ), was approximated as the mass ratio assuming the gel density is constant.

SAXS measurements were performed using a linearly collimated Kratky compact small-angle system equipped with a position sensitive detector (OED 50 M from MBraun, Graz, Austria). Incident radiation of wavelength  $\lambda = 1.542 \text{ \AA}$  (Cu K $\alpha$ ) was provided by a Seifert IF 300 X-ray generator operating at 50 kV and 40 mA. The sample to detector distance was 277 mm. The scattered signal was distributed over 1024 channels 53  $\mu\text{m}$  in width. The center beam channel was determined between every sample measurement to ensure accurate assignment of the scattering peak positions. Gel samples and a drop of the external equilibrated surfactant solution were sealed between two mica slides in the sample holder. The angle between the incident and scattered radiation,  $2\theta$ , is related to the scattering vector,  $q$ , and the corresponding spacing between reflecting planes,  $d$ , by Bragg's law,  $d^{-1} = q/2\pi = (2/\lambda)(\sin \theta)$ . The unit cell dimension is  $l = d(h^2 + k^2 + l^2)^{1/2}$ , where  $h$ ,  $k$ , and  $l$  are the Miller indices of the reflecting planes.

The equilibrated aqueous DTAB concentration was determined using a surfactant specific membrane electrode as described in ref 10. The electrode response to DTAB was Nernstian with a slope of 58 mV per decade change in concentration, so long as the surfactant concentration lies below the mixture cmc. To ensure this criterion is met, solutions for analysis were diluted below the cmc of the surfactant solution as initially prepared. In addition, a small volume of support electrolyte was added to each test solution so that the concentration of NaCl was 50 mM. Three analyte solutions at different dilutions were prepared from each gel

\* To whom correspondence should be addressed. Present address: Princeton University, Department of Chemical Engineering, The Engineering Quadrangle, Olden St., Princeton, NJ 08544-5263. E-mail: hank@princeton.edu.

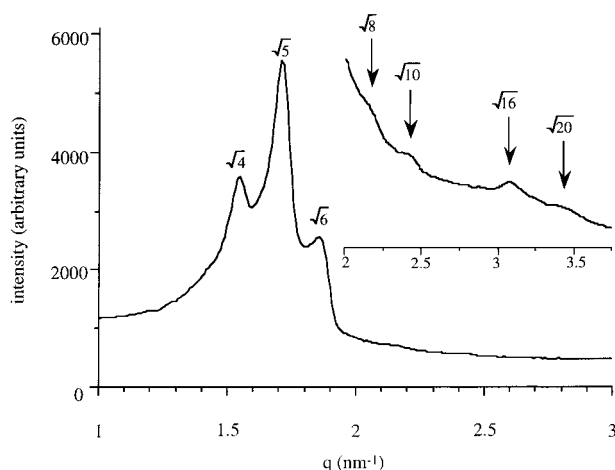


**Figure 1.** SAXS spectrum of neat cPA-DTA<sup>+</sup> complex. The peak indices  $(h^2 + k^2 + l^2)^{1/2}$  are indicated. The inset figure shows the weaker structure observed at high  $q$  in detail. This structure is consistent with the  $Pm\bar{3}n$  space group with a unit cell dimension of 8.21 nm.

sample. The electrode was left in contact with the analyte solution for 10–15 min before a measurement was taken to ensure equilibration for accurate concentration measurement. This is especially important for the most concentrated solutions which require the greatest dilution to get below the mixed cmc and required longer electrode equilibration times. The aqueous DTAB concentration was determined as the average of the three solutions, and a standard error was calculated.

The aqueous C<sub>12</sub>E<sub>8</sub> concentration in the external aqueous solutions was determined by <sup>1</sup>H NMR following the evaporation and redissolution in d-DMSO (Aldrich) procedure described in ref 9. Spectra were recorded on a Bruker DRX500 NMR spectrometer (resonance frequency of 500.13 MHz). The external aqueous surfactant fractions of C<sub>12</sub>E<sub>8</sub> to DTAB was determined from the ratio of peaks and the C<sub>12</sub>E<sub>8</sub> concentration evaluated using the DTAB concentration measured potentiometrically.

## Results and Discussion

To begin, the neat cPA-DTA<sup>+</sup> complex structure is characterized by SAXS (Figure 1). Three dominant peaks are observed at low  $q$  with ratios of  $4^{1/2}:5^{1/2}:6^{1/2}$  indicating a primitive cubic structure with a unit cell dimension of  $l = 8.21$  nm, similar in structure to that observed for dodecylpyridinium chloride–polyacrylamide-methylpropanesulfonic acid gel complexes.<sup>5</sup> Four less prominent peaks are observed at higher  $q$  (Figure 1 inset) whose peak indices are consistent with the  $Pm\bar{3}n$  space group<sup>11</sup> assigned by Chu and co-workers for the DTA<sup>+</sup>–poly(methacrylic acid) gel complex.<sup>3</sup> On the basis of SAXS and time-resolved fluorescence quenching measurements (TRFQ), Hansson determined that there are six micelles per unit cell for the DTA<sup>+</sup>–cPA complex.<sup>4</sup> Assuming six micelles per unit cell, we calculate a DTA<sup>+</sup> aggregation number of 85 from the gel collapse and surfactant absorption results presented below, comparable to Hansson's TRFQ measurements. An idealized spherical DTA<sup>+</sup> micelle has an aggregation number of 55.<sup>12</sup> Thus, we conclude the absorbed aggregates are elongated with an axial ratio of 1.4 assuming a rodlike shape.

The evolution of the surfactant–gel complex structure with increasing C<sub>12</sub>E<sub>8</sub> concentration is shown in Figure 2. Primarily, C<sub>12</sub>E<sub>8</sub> melts the cubic structure of the cPA-DTA<sup>+</sup> complex leaving only a single broad scattering peak for C<sub>12</sub>E<sub>8</sub> concentrations greater than about 4 mM. Thus, reduction of bound micelle charge density

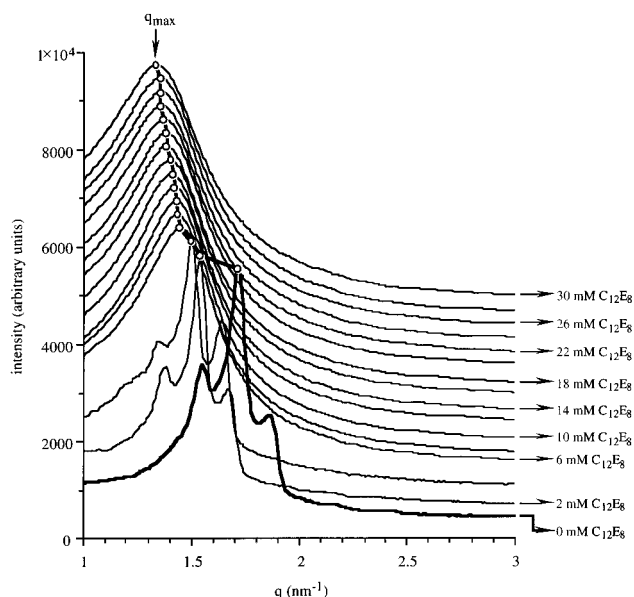


**Figure 2.** SAXS spectra of the cPA-mixed surfactant complexes as a function of increasing C<sub>12</sub>E<sub>8</sub> concentration. The spectra are shifted upward with increasing initial aqueous C<sub>12</sub>E<sub>8</sub> concentration, indicated on the right-hand side. The bold curve at the bottom is the neat cPA-DTA<sup>+</sup> spectrum. The open circles follow the maximum peak position,  $q_{\max}$ .

by nonionic surfactant incorporation diminishes the interaction strength and correlations between aggregates. The peak maximum occurs at  $q$  values close to  $\sim 1.4$  nm<sup>−1</sup>, corresponding to a length of 4.5 nm. This spacing is a little greater than the diameter of a DTAB micelle, so we attribute this peak simply to the bound intermicellar spacing. Following the position of the maximum scattering peak with increasing C<sub>12</sub>E<sub>8</sub> concentration, either the  $5^{1/2}$  reflection for the cubic complexes or the maximum for the unstructured complexes, we find that  $q_{\max}$  shifts to lower values with increasing nonionic surfactant concentration (Figure 2). That is, as C<sub>12</sub>E<sub>8</sub> is added, the dominant correlation length increases and the complex structure swells. While the complexes may swell simply by the added volume of the nonionic surfactants, this is unlikely since nonionic surfactant absorption appears to be constant over the C<sub>12</sub>E<sub>8</sub> concentrations examined as shown below.

The volume collapse ratio, plotted as a function of C<sub>12</sub>E<sub>8</sub> concentration in Figure 3, provides a second measure of length in the gels. Neat DTA<sup>+</sup> collapses the gel by nearly 2 orders of magnitude,  $a_0^{-1} = 71$ , while addition of C<sub>12</sub>E<sub>8</sub> swells the complex by a factor of up to 2.5. More interestingly, however, the gels swell in discrete steps at initial nonionic surfactant concentrations of approximately 17, 23, and 29 mM, between which  $\alpha$  is constant (Figure 3a). The gel collapse results at the same initial nonionic surfactant conditions from ref 9 are in good agreement with those measured presently (Figure 3a), indicating that they are reproducible. These previous results, however, do not capture the present swelling steps because they were measured at more widely spaced C<sub>12</sub>E<sub>8</sub> concentrations. A quantitative comparison of the macroscopic swelling of the gel and the microscopic structure can be made by cubing the SAXS correlation length to obtain a volume, as shown in Figure 3b where  $\alpha$  and  $q_{\max}$  are scaled relative to the neat cPA-DTA<sup>+</sup> complex. For C<sub>12</sub>E<sub>8</sub> concentrations less than 17 mM the macroscopic and microscopic swelling of the surfactant–gel complex track one another almost

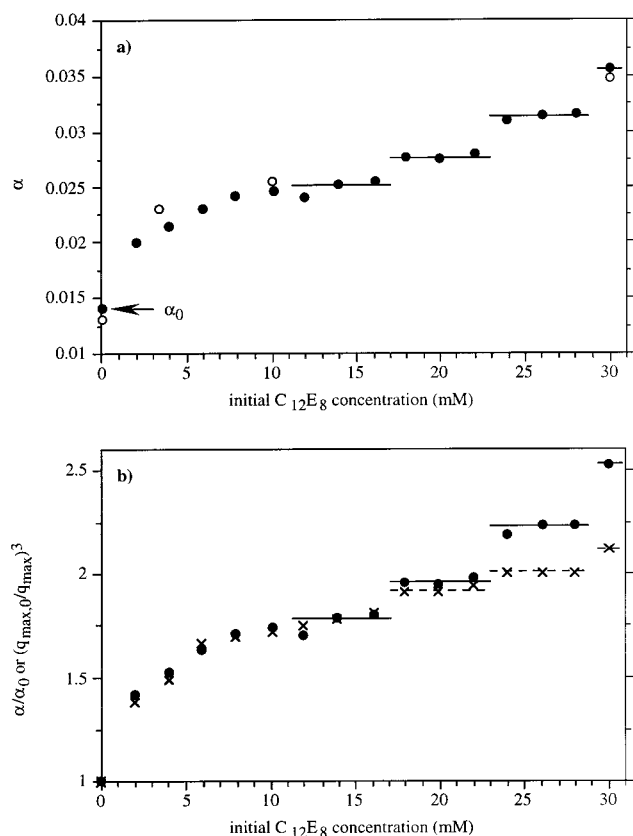


**Figure 3.** (a) Volume collapse ratio as a function of the initial aqueous phase  $C_{12}E_8$  concentration. The closed circles denote the collapse ratios measured presently, while the open circles are taken from ref. 9. The horizontal lines indicate the swelling steps discussed in the text. (b) Comparison between the volume collapse ratio and the SAXS correlation length  $(1/q_{\max})^3$  scaled by their neat cPA-DTA<sup>+</sup> values. The filled circles denote the mass collapse ratios, while the crosses denote the SAXS correlation lengths.

perfectly. Thus, the increase in the SAXS correlation length with increasing  $C_{12}E_8$  is manifested as an isotropic macroscopic swelling of the gel. Moreover, when the gel undergoes macroscopic swelling steps the SAXS correlation length increases discontinuously as well. The discontinuous decrease in  $q_{\max}$ , however, is subtle and not as significant as the macroscopic swelling of the complex. In addition, the disparity between the microscopic and macroscopic swelling increases with further  $C_{12}E_8$  addition. We conclude that the step swelling of the complex volume occurs on a length scale greater than that of the individual micelles and greater than that probed by SAXS. This observation suggests that the gel forms micelle-rich domains separated by aqueous micelle-lean domains that crack open at each swelling step.

While we do not have a definitive explanation of these stepwise swelling transitions, surfactant absorption measurements have been performed to obtain further clues into the origin of this unexpected behavior. The DTA<sup>+</sup> and  $C_{12}E_8$  absorption fractions, defined as the total amount of surfactant absorbed by the gel divided by the total number of cPA monomers ( $\beta_{DTA^+}$  or  $\beta_{C_{12}E_8}$ ), are plotted in Figure 4. The neat cPA-DTA<sup>+</sup> system forms a one-to-one complex,  $\beta_{DTA^+} = 1$ , neutralizing the gel. DTA<sup>+</sup> absorption decreases approximately linearly with  $C_{12}E_8$  concentration up to the first swelling transition, after which  $\beta_{DTA^+}$  assumes a more or less constant value,  $\beta_{DTA^+} \approx 0.6$ . The decrease in  $\beta_{DTA^+}$  can explain

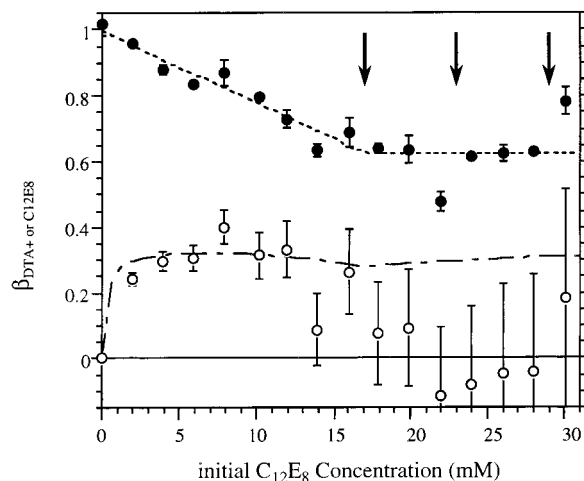


**Figure 4.** Surfactant absorption fractions as a function of the initial aqueous phase  $C_{12}E_8$  concentration. The filled circles denote the measured DTA<sup>+</sup> absorption, while the open circles denote the measured  $C_{12}E_8$  absorption. The DTA<sup>+</sup> error bars are the standard deviation in  $\beta_{DTA^+}$  calculated from three separate samples. The  $C_{12}E_8$  error bars are calculated for an error of  $\pm 0.005$  in the aqueous  $C_{12}E_8$  surfactant fraction determined by NMR. The vertical arrows indicate the swelling step concentrations observed in Figure 3. The short dashed line is a guide for the eye drawn through the  $\beta_{DTA^+}$  results showing the decreasing and plateau absorption regimes. The long-short dashed line is the model prediction for  $\beta_{C_{12}E_8}$  following the short dashed line for  $\beta_{DTA^+}$  and using  $C_1^{g*} = 0.25$  mM.

the swelling of the gel complex at low to moderate  $C_{12}E_8$  concentrations, in part, by the increased internal osmotic pressure of the mobile sodium counterions retained to maintain gel electroneutrality.

The corresponding absorption of  $C_{12}E_8$  is essentially independent of  $C_{12}E_8$  concentration,  $\beta_{C_{12}E_8} \approx 0.3$ , over the range DTA<sup>+</sup> absorption decreases. For high  $C_{12}E_8$  concentrations the measured  $\beta_{C_{12}E_8}$  drops and physically unrealistic negative values are observed. The measured  $\beta_{C_{12}E_8}$  becomes increasingly unreliable with increasing  $C_{12}E_8$  concentration, however, owing to the uncertainties in the aqueous  $C_{12}E_8$  surfactant concentration determined by NMR in combination with the evaluation of small  $\beta_{C_{12}E_8}$  from the difference between large initial and equilibrium aqueous  $C_{12}E_8$  concentrations. Assuming an error of  $\pm 0.005$  in the aqueous  $C_{12}E_8$  surfactant fraction from control NMR measurements, increasing errors in  $\beta_{C_{12}E_8}$  are observed which are larger than  $\beta_{C_{12}E_8}$  at the highest  $C_{12}E_8$  concentrations examined (Figure 4).

To obtain a better estimate of  $\beta_{C_{12}E_8}$  over the entire concentration range, we have modified a mass action model, previously developed to describe mixed ionic/nonionic surfactant absorption by an oppositely charged gel, to describe the equilibrium aqueous/gel phase partitioning of the nonionic surfactant given that the ionic surfactant absorption is known.<sup>9,13</sup> DTA<sup>+</sup> absorption fractions used in the model are taken from the short dashed line drawn in Figure 4 following  $\beta_{DTA^+}$  simply to obtain a smooth correlation for  $\beta_{C_{12}E_8}$ . The model, fitted to  $\beta_{C_{12}E_8}$  for  $C_{12}E_8$  concentrations up to 6 mM, describes the experimental  $C_{12}E_8$  absorption well up to moderate concentration. Extrapolated over the entire concentration range examined, the model predicts  $\beta_{C_{12}E_8}$  is essentially constant and equal to  $\sim 0.3$ . Thus, it appears that  $C_{12}E_8$  absorption plays only a minor role in the swelling of the gel complex. Moreover, since  $\beta_{DTA^+}$  and



$\beta_{C_{12}E_8}$  are constant above the first swelling step, it is unlikely that the net surfactant charge or micelle surface charge density play a role in these transitions, consistent with the conclusion above that this swelling originates on a length scale greater than that of an individual micelle.

Since surfactant absorption does not appear to change above the first swelling step it is unlikely this swelling can be attributed to changes in micelle charge within the gel. Rather, swelling could result from a reduction in external osmotic pressure exerted by the aqueous bath. The neat DTAB solution consists of unaggregated  $DTA^+$  and  $Br^-$  counterions below the cmc ( $cmc_{DTAB} = 15$  mM).  $C_{12}E_8$  is added above its cmc ( $cmc_{C_{12}E_8} = 0.1$  mM) and thereby contributes little to the external osmotic pressure. Moreover, as the  $C_{12}E_8$  concentration is increased, DTAB monomers are swept up from bulk solution into mixed micelles thereby reducing the external osmotic pressure by reduction of the  $DTA^+$  monomer population and  $Br^-$  condensation on mixed micelle surfaces. As a result, the surfactant–gel complex swells with increasing  $C_{12}E_8$  concentration. The step-wise nature of the swelling is reminiscent of the incremental swelling of hydrated clays, although this comparison may only be facile given the structural differences between clays and our complexes.<sup>15,16</sup> Nonetheless, multiple discrete swelling transitions have been observed for polyampholytic gels, which are more closely related chemically to our gel–surfactant complexes.<sup>17</sup> Another possibility is that there is a two phase equilibrium between surfactant liquid crystalline phases trapped within the gel, although the present diffraction results do not lend supporting evidence. Our observations suggest that the external solution conditions is an important variable with which surfactant–gel mesostructure can be tuned. This hypothesis can be tested by examining the effect of a nonabsorbing stressing polymer, such as poly(ethylene glycol), on recompression of the complexes. Moreover, the heterogeneous structure of the swollen gel complexes could be examined by self-diffusion NMR measurements of probe mobility within the swollen complexes.

**Acknowledgment.** The authors wish to thank Karl-Erik Bergquist who performed the NMR measurements. We also thank Per Hansson, Andrew Fogden, and Lennart Piculell for helpful suggestions and discussions. This work was supported by the Center for Amphiphilic Polymers from Renewable Resources, Lund University.

## References and Notes

- (1) Ober, C. K.; Wegner, G. *Adv. Mater.* **1997**, *9*, 17.
- (2) Hansson, P.; Lindman, B. *Curr. Opin. Colloid Interface Sci.* **1996**, *1*, 604.
- (3) Zhou, S.; Burger, C.; Yeh, F.; Chu, B. *Macromolecules* **1998**, *31*, 8157.
- (4) Hansson, P. *Langmuir* **1998**, *14*, 4059.
- (5) Okuzaki, H.; Osada, Y. *Macromolecules* **1995**, *28*, 380.
- (6) Sokolov, E. L.; Yeh, F.; Khokhlov, A.; Chu, B. *Langmuir* **1996**, *12*, 6229.
- (7) Yeh, F.; Sokolov, E. L.; Khokhlov, A. R.; Chu, B. *J. Am. Chem. Soc.* **1996**, *118*, 6615.
- (8) Hansson, P.; Schneider, S.; Lindman, B. *Prog. Colloid Polym. Sci.* **2000**, *115*, 342.
- (9) Ashbaugh, H. S.; Piculell, L.; Lindman, B. *Langmuir* **2000**, *16*, 2529.
- (10) Hayakawa, K.; Kwak, J. C. T. *J. Phys. Chem.* **1982**, *86*, 3866.
- (11) *International Tables for X-ray Crystallography*; Kynoch Press: Birmingham, U.K., 1952.
- (12) Tanford, C. *The Hydrophobic Effect: Formation of Micelles and Biological Membranes*, 2nd ed.; John Wiley & Sons: New York, 1980.
- (13) Previously we developed a mass-action model describing the absorption of both nonionic (component 1)/cationic (component 2) surfactant mixtures by an anionic gel, described in detail in ref 9. This model can be simplified to describe the absorption of the nonionic surfactant alone assuming the absorption of the cationic surfactant is known. Since the gel and nonionic surfactant do not interact strongly, absorption of this component is thought to proceed by mixed micellization with the cationic surfactant in the gel phase. Three steps are essential for describing absorption: *Mixed micellization in the aqueous phase*. As the surfactant concentrations in the aqueous phase typically lie above the mixed cmc this process must be taken into account. Assuming ideal mixing the aqueous concentration of nonionic surfactant monomers,  $C_{1m}^w$ , is<sup>14</sup>

$$C_{1m}^w = C_1^w - (C_{12}^w - \Delta) + [(C_{12}^w - \Delta)^2 + 4y_1 C_{12}^w \Delta]^{1/2} / 2\Delta \quad (1)$$
where  $C_{12}^w$  is the total surfactant concentration in the aqueous phase,  $C_1^*$  is the aqueous cmc of the nonionic surfactant,  $\Delta = C_2^* - C_1^*$  the difference between the cmc's of the pure surfactants, and  $y_1$  is the aqueous nonionic surfactant fraction. *Mixed micellization in the gel phase*. In analogy to aqueous mixed micellization, gel phase aggregation is assumed ideal. In this case, it can be shown that the concentration of nonionic monomers in the gel phase,  $C_{1m}^g$ , is
$$C_{1m}^g = x_1 C_1^g \quad (2)$$
where  $x_1$  is the mole fraction of nonionic surfactants in gel bound aggregates, and  $C_1^g$  is the gel phase critical aggregation concentration of the nonionic surfactant. All the cationic surfactant absorbed by the gel is assumed to be aggregated which is reasonable at the experimental  $DTA^+$  absorption fractions. *Surfactant monomer partitioning between phases*. The gel and aqueous phases are coupled to one another by the nonionic surfactant monomer concentrations in either phase, which are assumed to be equal at equilibrium
$$C_{1m}^w = C_1^g \quad (3)$$
with no correction for solution nonidealities. The aqueous cationic and nonionic surfactant cmc's are set equal to their experimental values of 15 and 0.1 mM, respectively. The cationic surfactant concentration in the aqueous and gel phases are set to the experimentally determined values and are used in evaluation of total surfactant concentrations and mole fractions in eqs 1 and 2. Thus,  $C_1^{g*}$  is the only fitting parameter. The value used is  $C_1^{g*} = 0.25$  mM, in reasonable agreement with the value of 0.20 mM from ref 9 fitted over a wider range of DTAB and  $C_{12}E_8$  concentrations.
- (14) Clint, J. H. *J. Chem. Soc., Faraday Trans. 1* **1975**, *71*, 1327.
- (15) Norrish, K. *Discuss. Faraday Soc.* **1954**, *18*, 120.
- (16) Dios Cancela, G.; Huertas, F. J.; Romero Taboada, E.; Sanchez-Rasero, F.; Hernandez Laguna, A. *J. Colloid Interface Sci.* **1998**, *185*, 343.
- (17) Annaka, M.; Tanaka, T. *Nature* **1992**, *355*, 430.

MA001545G